Available online at www.sciencedirect.com
SCIENCE DIRECT
Physica C 436 (2006) 62–67
PHYSICA C
www.elsevier.com/locate/physc

In situ high temperature optical microscopy study of phase evolution in $YBa_2Cu_3O_{7-\delta}$ films prepared by a fluorine-free sol–gel route

Yulong Zhang [a], Xin Yao [a], Jie Lian [b], Lumin Wang [b], Aihua Li [c], H.K. Liu [c], Haibo Yao [d], Zhenghe Han [d], Laifeng Li [e], Yongli Xu [f], Donglu Shi [f,*]

[a] *Department of Physics, State Key Laboratory for Metal Matrix Composites, Shanghai Jiao Tong University, Shanghai, China*
[b] *Department of Nuclear Engineering and Radiological Science, University of Michigan, Ann Arbor, MI 48109, United States*
[c] *Institute of Superconducting and Electronic Materials, University of Wollongong, Wollongong, NSW, Australia*
[d] *Applied Superconductivity Research Center, Tsinghua University, Beijing, China*
[e] *Technical Institute of Physics and Chemistry, Chinese Academy of Sciences, Beijing, China*
[f] *Department of Chemical and Materials Engineering, University of Cincinnati, Cincinnati, OH 45221-0012, United States*

Received 6 September 2005; received in revised form 4 January 2006; accepted 12 January 2006
Available online 9 March 2006

Abstract

Phase evolution of $YBa_2Cu_3O_{7-\delta}$ (YBCO) thin films prepared by a newly-developed fluorine-free sol–gel method were studied by combined use of in situ high temperature optical microscope observation and X-ray diffraction. The reaction sequences associated with yttrium, barium and copper in this route were determined respectively. It was found that the reactions that take place were strongly dependent on the experimental conditions such as water partial pressure. The formation of YBCO started around 710 °C and continued up to 800 °C for about 15 min. The formation mechanism of YBCO was found to be dependent on the barium containing phases, which were controlled by the experimental conditions. The formation of *a*- and *c*-axes oriented YBCO grains was also found to be governed by the processing reactions.

1. Introduction

As a promising method, trifluoroacetate (TFA) metall-organic deposition (MOD) has successfully fabricated $YBa_2Cu_3O_{7-\delta}$ (YBCO) films with J_c over 1 MA/cm^2 at 77 K on both single crystal substrate and buffered metallic substrates of RABiTS [1,2]. The TFA-MOD approach has several advantages over vapor deposition methods, particularly in the industrial applications including low cost and continuous process. Trifluoroacetate salts have been found to avoid the formation of stable $BaCO_3$ at the grain boundaries because of its lower stability than barium fluoride [2].

Although fluorine can be removed in the form of HF through heat treatment at high temperatures (>650 °C) in humid, low oxygen partial pressure atmosphere, it is a non-trivial process. Moreover, there are issues related to fluid flow and complicated reactor designs that may be required for scale-up. Recently, a fluorine-free sol–gel approach involving the trimethylacetate salts and propionic acid (TMAP) precursor solution has been developed and a high transport J_c was obtained on the order of 1 MA cm^{-2} at 77 K [3–6]. It provides an alternative method for fabricating long-length conductors in large-scale applications, in which no fluorine-containing compounds including HF, BaF_2 are formed. In addition, the films prepared by the TMAP-MOD approach possess much denser microstructures compared to TFA films, and the TMAP precursor solution is stable for several months [4]. The processing route has been established in previous studies and high-quality YBCO films can be synthesized by this newly-developed, fluorine-free TMAP method for coated conductor development. It is believed that carbon could be removed from the materials at low

* Corresponding author. Tel.: +1 513 5563100; fax: +1 513 5562569.
E-mail address: donglu.shi@uc.edu (D. Shi).

0921-4534/$ - see front matter © 2006 Elsevier B.V. All rights reserved.
doi:10.1016/j.physc.2006.01.038

temperature burnout stage (<400 °C) in wet oxygen [4]. The superconducting properties and resultant microstructures of prepared films are found to be strongly correlated with parameters such as oxygen and water partial pressures and resultant microstructures [4–7].

In order to control the TMAP-MOD process and to optimize the superconducting properties of the films, it is crucial to understand the detailed mechanism and the related chemistry of the formation of YBCO. In this current work, in situ high temperature optical microscopy and ex situ X-ray diffraction are applied to study the development of the intermediate crystalline phases during the conversions in the TMAP-MOD process. The phase evolution and the mechanism of YBCO formation during the TMAP-MOD approach are discussed.

2. Experimental

The fluorine-free sol–gel solutions were developed in-house. The precursor solutions were prepared by the following procedure: stoichiometric (1:2:3) $Y(C_4H_9COO)_3$ (yttrium trimethylacetate), $Ba(C_4H_9COO)_2$, and $Cu(C_4H_9COO)_2$ were dissolved into propionic acid and amine solvents, forming a dark green solution with an oxide concentration between 0.1 and 0.5 mol l^{-1}. The presence of amine improved the solubility of the precursor powders in propionic acid. After filtration, the precursor solution was deposited onto the substrates by a spin-coater at a speed of 2000–5000 rpm. The multi-coatings with the intermediate baking procedure at 200–250 °C were performed on a hot plate to make thicker films. The samples were burn out in a quartz furnace under humid 200 ppm oxygen at 400 °C for 10 h, and the dew point was 20 °C. Afterward, the intermediate films were subject to a high temperature anneal at 745 °C with a speed of 25 °C min^{-1}, then to 750 °C at the rate of 1 °C min^{-1}, dwelling at 750 °C for 80 min. Ten minutes before the end of the dwelling process, the furnace atmosphere was switched to dry, and the temperature was decreased to 450 °C at the rate of 2.5 °C min^{-1}. After oxygenating for 60 min in flowing oxygen, the samples were furnace-cooled to room temperature. Substrates used in this experiment were commercial LAO and MgO single crystals with the (0 0 1) orientation. The LAO single crystals had dimensions of $12 \times 12 \times 1$ mm^3 and were purchased from MTI Company. One side of the single crystal was polished as-purchased. The average thickness of the films was about 80 nm.

The in situ observations were conducted on a high temperature optical microscope (HTOM, OLYMPUS BX51M). The intermediate spin-coated films were used on the observation under the atmosphere of $99\%N_2 + 1\%O_2$. The heating program was as follows: heating up to 400 °C and dwelling for 10 min, and then to 800 °C with a speed of 100 °C min^{-1}. To prepare the samples for XRD and EDS, the films were cooled to room temperature from a given temperature, such as 550 °C and 650 °C. The cooling rate was set at 130 °C min^{-1}, close to the rate of air-quenching. The phases identified by X-ray diffraction (XRD, D8 Discover GADDS diffractometer, Cr radiation) and EDS detecting unit connected to a PHILIPS515 scanning electric microscope (SEM) were regarded as the intermediate ones at these temperatures during the phase evolution. The high-resolution TEM (HRTEM) experiments were performed on a JEOL JEM 4000EX TEM. Transport resistivity measurements were carried out down to liquid-helium temperature using a standard four-probe method.

3. Results and discussion

As mentioned above, the TMAP-MOD process can be divided into two steps, i.e. burnout and high temperature conversions. The first step of burnout mainly involves the removal of organic materials such as solvents and hydrocarbons in metallorganic salts. The precursor solution is composed of $Ba(C_2H_5COO)_2$, $Y(C_2H_5COO)_3$, $Cu(C_2H_5COO)_2$, C_2H_5COOH, C_4H_9COOH, $C_4H_9CONHC_5H_{11}$ and H_2O. The boiling points of propionic acid and amylamine were at 141 °C and 104 °C, respectively [5]. In the baking stage, the extra C_2H_5COOH, C_4H_9COOH, and water were evaporated at around 150 °C.

Figs. 1 and 2 show the intermediate phases and the phase development during the process. The main changes of the microstructures were observed at around 490 °C, 550 °C, and 650 °C through HTOM, and the YBCO began to form at about 710 °C. As can be seen in Fig. 1(a), no noticeable changes can be observed on HTOM until 490 °C.

The pyrolysis processes take place in the burnout stage. However, only two peaks of the monoclinic $BaCO_3$ can be index at 400 °C in Fig. 2. There are no peaks involving with Y compound. The possible reason is that it exists in an amorphous or nano-size form and could not be detected by XRD.

As far as the barium-related phases are concerned, there are two metastable compounds, i.e. $Ba(OH)_2 \cdot 8H_2O$ and $BaCO_3$. Xu [5] found that the conversions for barium-related phases were strongly dependent on the water vapor partial pressure. $Ba(OH)_2 \cdot xH_2O$ was formed between 220 and 310 °C under a dry atmosphere through the following reactions:

$$2C_2H_5COOH + O_2 \rightarrow CO_2 + H_2O \quad (1)$$

$$Ba(C_2H_5COO)_2 + xH_2O \rightarrow Ba(OH)_2 \cdot xH_2O + 2C_2H_5COOH \quad (2)$$

The x value is less than 8, signifying water deficiency, which increases the melting point of $Ba(OH)_2 \cdot xH_2O$ above 310 °C. On the other hand, when the precursor films are exposed to water, the reaction product is $Ba(OH)_2 \cdot 8H_2O$:

$$Ba(C_2H_5COO)_2 + 9H_2O \rightarrow 2C_2H_5COOH + Ba(OH)_2 \cdot 8H_2O \quad (3)$$

It was suggested that $BaCO_3$ was formed at about 350 °C through the reaction below [5]:

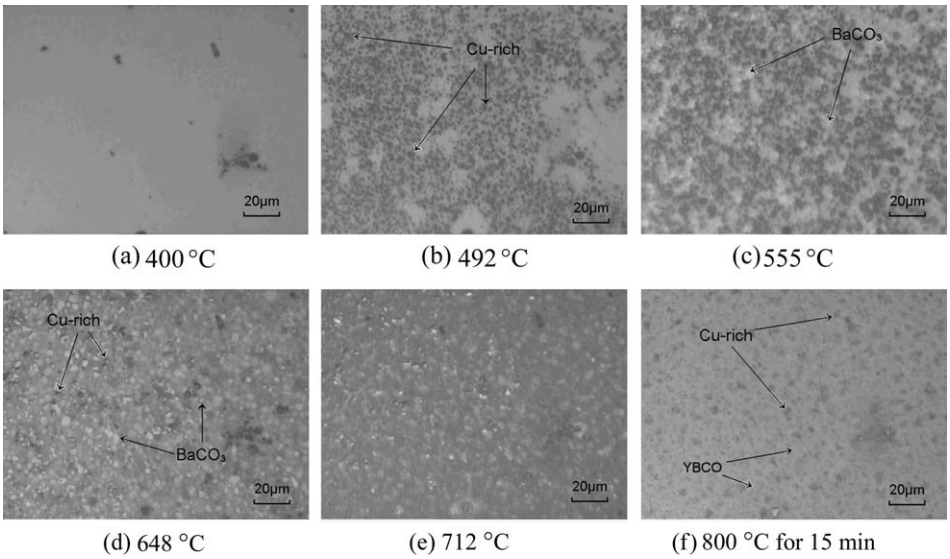

Fig. 1. The microstructural evolution of the YBCO film observed by HTOM.

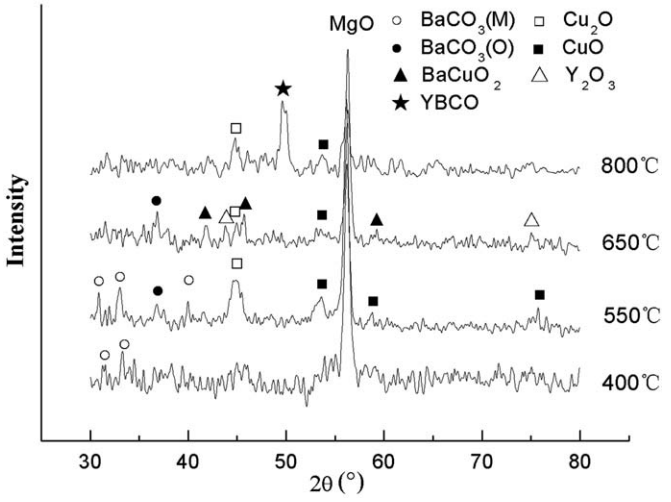

Fig. 2. XRD patterns for quenched films.

$$Ba(OH)_2 \cdot 8H_2O + CO_2 \rightarrow BaCO_3 + 9H_2O. \quad (4)$$

Some peaks of $BaCO_3$ were also found in samples quenched from 400 °C under dry atmosphere and no liquid phases were found in HTOM observations. This means that $BaCO_3$ can form in a dry atmosphere even though $Ba(OH)_2 \cdot xH_2O$ may be less reactive with CO_2 than $Ba(OH)_2 \cdot 8\,H_2O$. XRD patterns in Fig. 2 show that the resultant $BaCO_3$ phase has a monoclinic crystal structure. In a humid furnace atmosphere, $BaCO_3$ is reacted with H_2O reversely [5]:

$$BaCO_3 + H_2O \rightarrow Ba(OH)_2 + CO_2\uparrow \quad (5)$$

Therefore, for the Ba(TMA) in the precursor solution, the final reaction product may be $BaCO_3$ or $Ba(OH)_2$, depending on the different furnace atmosphere.

Fig. 1(b) shows that at about 490 °C, the conversions take place rapidly and a large amount of spherical particles emerge. As the temperature increases to about 550 °C, the particles grow considerably and cover the whole surface of the film. Meanwhile, some black particles, the Cu-rich phases determined by EDS, were observed to turn brown and then yellow gradually, demonstrating an oxidation process of Cu-containing phases.

The 550 °C quenched films are composed of monoclinic and orthorhombic $BaCO_3$, Cu_2O and CuO, as shown in Fig. 2. There exist no peaks of Y compounds still for the reason mentioned above. The occurrence of some orthorhombic $BaCO_3$ indicates an allotropic transformation from monoclinic. The low relative intensity of the orthorhombic $BaCO_3$ peak means the beginning of this transformation, which was found at about 400 °C in Ref. [5]. A process of oxidation for $Cu(TMA)_2$ precursor was suggested [5]:

$$Cu(C_2H_5COO)_2 \overset{190\ ^\circ C}{\rightarrow} Cu \overset{220\ ^\circ C}{\rightarrow} Cu_2O \overset{310\ ^\circ C}{\rightarrow} CuO \quad (6)$$

The resultant pure copper in an oxidation atmosphere resulted from the locally reducing atmosphere formed during heating up when vast amount of organic compounds decomposed [5]. The above oxidation sequence were also observed in the BaF_2 conversion process except for the pyrolysis of $Cu(C_2H_5COO)_2$ [8]. However, the amorphous pure copper was reported to be oxidized first to Cu_2O around 400 °C, and then to CuO at about 550 °C [8]. In our HTOM observations, the copper-related phases with different colors may represent Cu, Cu_2O and CuO, respectively, although further confirmation is needed. The deviation of the reaction temperatures may come from the different experimental procedures, especially the heating rate, although the temperature for the CuO formation in our experiments was observed to be close to that in Ref. [8].

At around 650 °C, a large amount of white particles appeared and the Cu-rich particles vanished. From the XRD pattern for the 650 °C quenched samples, four main

changes were observed: (1) the monoclinic $BaCO_3$ peaks vanish, indicating that all of the $BaCO_3$ transformed into orthorhombic phase; (2) two Y_2O_3 peaks appear; (3) $BaCuO_2$ peaks appear, and (4) the intensities of Cu_2O and CuO peaks become weaker than those at 550 °C.

The appearance of the yttrium-containing phase is ambiguous. In the TGA experiments by Xu [5], the decomposition product of $Y(TMA)_3$ precursor was identified as Y_2O_3 directly because the weight loss was in agreement with the theoretical value. The existence of Y_2O_3 could not be detected by XRD because of its amorphous or nano-sized form. Chu [9] reported that the crystallization of the Y_2O_3 phase may start from 400 °C. Thus, the detection of Y_2O_3 at 650 °C may be an evidence of the growth of Y_2O_3 grains rather than crystallization. It also indicates that Y_2O_3 is not involved with other reactions except for the decomposition until 650 °C.

Three diffraction peaks in Fig. 2 indicate the formation of $BaCuO_2$ phase. Chu suggested the reactions in $BaCuO_2$ and CuO system, and proposed the following reactions [10]:

$$BaCO_3 + CuO \rightarrow BaCuO_2 + CO_2 \tag{7.1}$$

$$BaCuO_2 + CuO \rightarrow L \tag{7.2}$$

$$Y_2O_3 + L \rightarrow YBCO \tag{7.3}$$

The $BaCuO_2$ phase might be formed through the reaction (7.1) because of the weaker intensities of CuO peaks. The reaction (7.3) took place at 640 °C in nitrogen and at 800 °C in air, as suggested by Chu [10]. It seemed that the formation of $BaCuO_2$ was closely related to the atmosphere. Few of liquid phases were found in either the HTOM observation or our previous experiments. The $BaCuO_2$ was very limited, and most of the barium source was in the form of $BaCO_3$. The reaction (7.3) was therefore not be the mechanism to form the highly *c*-axis oriented YBCO films with good superconducting properties.

About 710 °C, YBCO begins to form and the conversion continues until dwelling at 800 °C for 15 min, as shown in Fig. 1(e) and (f). Associating the conversion with different sources of barium, the formation of YBCO is suggested to undergo one of the following reactions:

$$4Ba(OH)_2 + 6CuO + Y_2O_3 \rightarrow 2YBa_2Cu_3O_{6.1} + xO_2 + 4H_2O\uparrow \tag{8}$$

$$4BaCO_3 + 6CuO + Y_2O_3 \rightarrow 2YBa_2Cu_3O_{6.1} + yO_2 + 2CO_2\uparrow \tag{9}$$

$$4BaO + 6CuO + Y_2O_3 \rightarrow 2YBa_2Cu_3O_{6.1} + zO_2 \tag{10}$$

where BaO can be form through the below reactions:

$$Ba(OH)_2 \rightarrow BaO + H_2O\uparrow \tag{10.1}$$

$$BaCO_3 + H_2O \rightarrow BaO + H_2CO_3\uparrow \tag{10.2}$$

$$BaCO_3 \rightarrow BaO + CO_2\uparrow \tag{10.3}$$

In previous studies, it was found that the relatively lower annealing temperature under humid atmosphere and low oxygen partial pressure suppresses *a*-axis growth, and the YBCO films prepared at high temperature were composed of *a*- and *c*-axes grains [4,5]. Assuming that the formations of *a*- and *c*-axes grains are governed by the same reaction, the nucleation and growth for the *a*- and *c*-axes YBCO are dominant at different temperature, because of the difference interfacial energy associated with substrates. And then the above experimental results indicate that the nucleation and growth for *c*- and *a*-axes grains take place at lower and higher temperatures, respectively. When heating at a very high speed, the nucleation and growth for *c*-axis grains will be suppressed. The reaction at lower temperature should not be observed on the surface of films under an optical microscope. However, in our HTOM observations, the formation of YBCO can take place in a large temperature range even though the heating rate is as high as 100 °C min^{-1}, implying that the different reactions are responsible for the formation of *a*- and *c*-axes grains.

Water is one of the reaction products in reaction (8), and cannot push this reaction to the right side. The formation mechanism of *c*-axis YBCO grains should follow reaction (8), since $Ba(OH)_2$ is the final product of Ba-containing phases in a humid atmosphere, and the films prepared only in a suitable water vapor pressure will exhibit the good superconducting properties [3–5]. While the atmosphere in furnace is dry or under a low water partial pressure, the mechanism to form YBCO should be operated by reaction (9) because BaO could not be detected in the quenched samples.

Another factor to influence the formation of YBCO is carbon dioxide as one of the reaction products in some reactions. Manabe et al. [11] investigated the carbon dioxide controlled annealing method for preparation of YBCO films by the dipping-pyrolysis process. In order to obtain highly *c*-axis oriented YBCO films, a three-step annealing method is proposed: first, high $p(CO_2)$; second, CO_2-free and low $p(O_2)$; and finally, CO_2-free and high $p(O_2)$. With this annealing method, contamination of *a*-axis grains was substantially prevented and highly *c*-axis YBCO films were obtained. They believed that the formation of YBCO grains from the precursor (Y_2O_3–$BaCO_3$–CuO) could be markedly suppressed under the high-$p(CO_2)$ environment during the heating ramp, at which temperatures *a*-axis grains tend to grow in the CO_2-free atmospheres. This experiment indicates that proposed reaction (9) is helpful to grow *a*-axis YBCO grains.

Therefore, it can be concluded that *c*-axis oriented grains are usually formed through reaction (8), while reaction (9) is responsible for the formation of mixed orientations (*a*- and *c*-axes) or polycrystalline grains when exposed to a dry atmosphere.

Similar YBCO samples developed by using the exact procedures described in the first paragraph of Section 2 were fully heat treated to obtain the *c*-axis oriented thin films. As previously reported [4], these films exhibit superb microstructures and superconducting properties. Fig. 3 shows a SEM micrograph of surface morphology of the

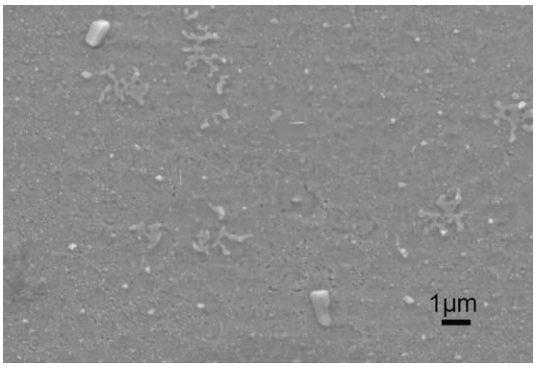

Fig. 3. SEM photographs of the surface morphologies of the *c*-axis oriented YBCO thin films.

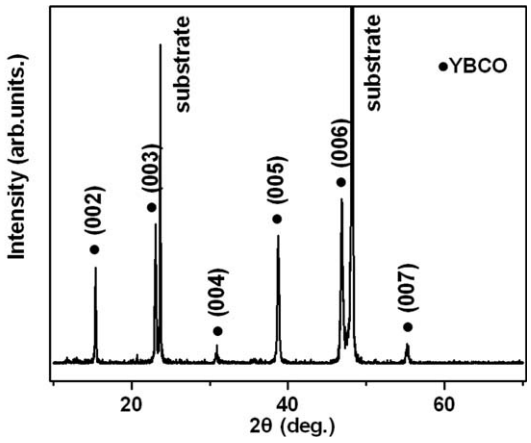

Fig. 4. XRD 2θ scan of the *c*-axis oriented YBCO thin film.

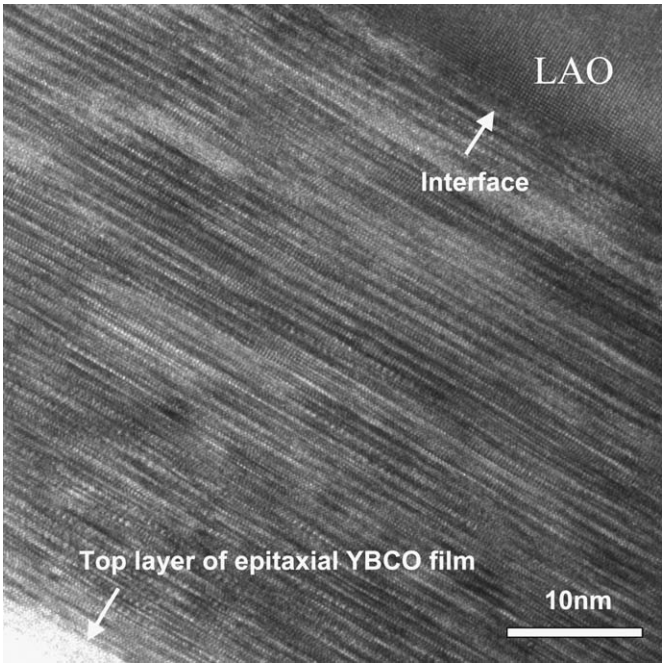

Fig. 5. HRTEM interface image of the *c*-axis oriented YBCO thin film.

fully heat treated, *c*-axis oriented YBCO thin film. Fig. 4 shows the XRD 2θ scan of the *c*-axis oriented YBCO film with all (00l) peaks indicating a well-textured grain structure. To further study the epitaxial structure of the YBCO thin films, HRTEM was performed on the film shown in Fig. 3. For the *c*-axis oriented thin film, the HRTEM revealed a coherent interface structure as shown in Fig. 5. In Fig. 5 the lattice image shows a clear lattice-matching interface between the LAO substrate and the YBCO phase. It was found out that this *c*-axis orientation extended all the way up to the film surface with a total thickness of 0.5 μm.

Fig. 6 shows the superconducting transitions by *ac* susceptibility (Fig. 6a) and transport resistivity (Fig. 6b) measurements for the *c*-axis oriented YBCO thin film. Quite sharp transitions take place at an onset value near 90 K. The transport J_c has been reported previously in YBCO films prepared by the same method. A high value on the order of $10^6 A/cm^2$ at 77 K and zero magnetic field has been

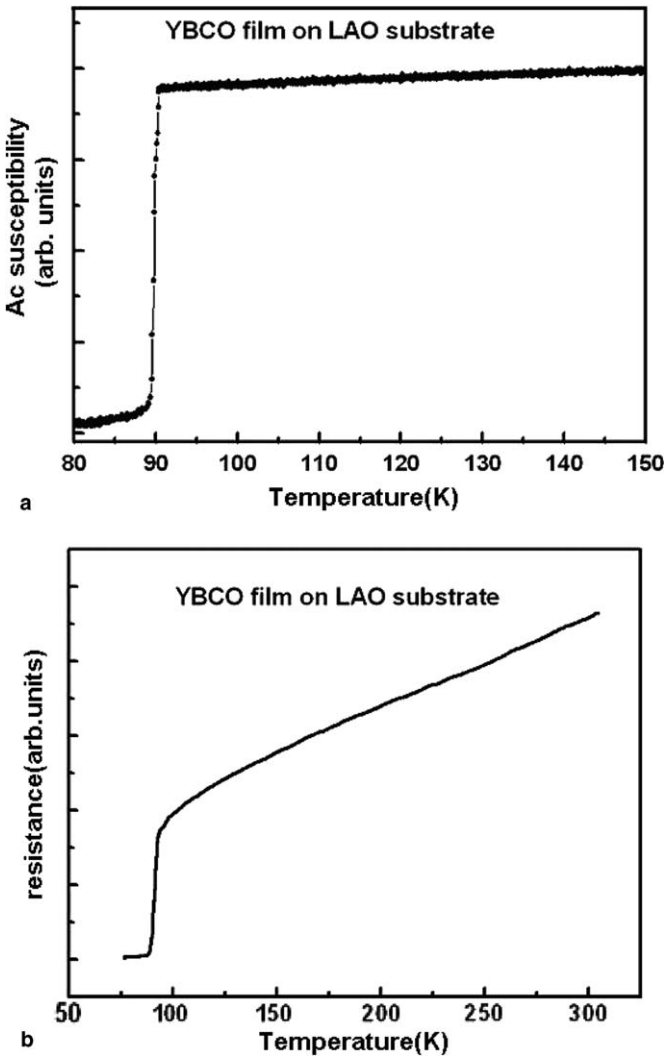

Fig. 6. (a) *ac* susceptibility and (b) resistivity versus temperature for the *c*-axis oriented YBCO film.

achieved [6]. This value is expected to improve as the processing parameters are further optimized.

4. Conclusion

In situ HTOM observation and XRD on quenched samples have been performed to analyze the phase evolution in YBCO films prepared by a fluorine-free TMAP-MOD method. The change of the barium phases is strongly dependent on temperature and water partial pressure. Monoclinic $BaCO_3$ is formed first after the pyrolysis in the burnout stage, and then transforms into orthorhombic phase up to 650 °C. As for the copper-containing phases, pure copper is the direct product from the decomposition of its precursor, which was then oxidized to Cu_2O and finally to CuO. Y_2O_3 grains grow considerably at about 650 °C and are not involved in any reactions before the formation of YBCO, although temperature for crystallization cannot be detected because of its amorphous or nano-sized nature. $BaCuO_2$ phase observed at 650 °C is not the dominated factor to control the YBCO formation. The formation mechanism of YBCO is dependent on the final reactant product of barium containing precursors, which is controlled by the experimental conditions. The *a*- and *c*-axes YBCO grains are suggested to be governed by reactions (8) and (9), respectively.

References

[1] T. Araki, H. Kurosaki, Y. Yamada, I. Hirabayashi, J. Shibata, T. Hirayama, Supercond. Sci. Technol. 14 (2001) 783.
[2] A.P. Malozemoff, S. Annavarapu, L. Fritzemeier, Q. Li, V. Prunier, M. Rupich, C. Thieme, W. Zhang, A. Goyal, M. Paranthaman, D.F. Lee, Supercond. Sci. Technol. 13 (May) (2000) 473.
[3] D.L. Shi, Y.L. Xu, S.X. Wang, J. Lian, L.M. Wang, S.M. McClellan, R. Buchanan, K.C. Goretta, Physica C 371 (2002) 97.
[4] J. Lian, H. Yao, D.L. Shi, L. Wang, Y.L. Xu, Q. Liu, Z. Han, Supercond. Sci. Technol. 16 (2003) 838.
[5] Y.L. Xu, High J_c epitaxial $YBa_2Cu_3O_{7-\delta}$ films through a non-fluorine approach for coated conductor applications, Ph.D dissertation, University of Cincinnati, December, 2003.
[6] Y. Xu et al., J. Mater. Res. 18 (3) (2003) 677.
[7] Y. Xu et al., J. Am. Ceram. Soc. 87 (9) (2004) 1669.
[8] W. Wong-Ng, I. Levin, R. Feenstra, L.P. Cook, M. Vaudin, Supercond. Sci. Technol. 17 (2004) s548.
[9] P.Y. Chu, in: Ceramic Engineering, University of Illinois at Urbana-Champaign, Urbana-Champaign, 1992.
[10] P.Y. Chu, R.C. Buchanan, J. Mater. Res. 9 (1993) 2134;
P.Y. Chu, R.C. Buchanan, J. Mater. Res. 9 (1994) 844.
[11] T. Manabe, I. Yamaguchi, S. Nakamura, W. Kondo, S. Mizuta, T. Kumagai, Physica C 276 (1997) 160.